Channel Parameter Estimation in Millimeter-Wave Propagation Environments Using Genetic Algorithm

Samuel Borges Ferreira Gomes ⬤, Nidhi Simmons ⬤, *Senior Member, IEEE*,
Paschalis C. Sofotasios ⬤, *Senior Member, IEEE*, Michel Daoud Yacoub ⬤, *Member, IEEE*,
and Simon L. Cotton ⬤, *Senior Member, IEEE*

Abstract—This letter explores the suitability of the nature-inspired genetic algorithm (GA) for estimating propagation channel parameters in an indoor millimeter-wave environment at 60 GHz. Our work is based on real propagation channel measurements and the goal is twofold: 1) to estimate physically plausible parameters; and 2) to provide improvements in terms of the goodness-of-fit when compared to traditional methods such as nonlinear least-squares (NLS). To better contextualize the use of the GA within the meta-heuristic family of algorithms, a more recent meta-heuristic approach, named the hybrid grey wolf and whale optimization algorithm (HGW-WOA), is also exercised. We adopt popular small-scale and shadowed-fading models which accurately characterize these mm-wave links. A total of 72 fading scenarios are investigated. The goodness-of-fit of these models, using different parameter estimation methods, is assessed through the Akaike information criterion. Our investigation has shown that the GA overwhelmingly outperformed the NLS. Similarly, the GA performed better than the HGW-WOA in the majority of scenarios. Thus, we demonstrate that the GA is a promising technique for the robust estimation of fading parameters.

Index Terms—Channel measurements, genetic algorithms, meta-heuristic algorithms, millimeter-wave communications.

I. INTRODUCTION

THE effective design and operation of wireless communication systems require a thorough understanding of the propagation characteristics of the operating environment [1]. This is especially true in millimeter-wave (mm-wave) communications, which will be integral to 6G. Propagation losses at mm-wave frequencies can be critical, leading to significant challenges in maintaining link reliability [2], [3]. Characterizing the fading conditions in these cases requires suitable channel models along with accurate parameter estimation methods. The method of moments and maximum likelihood estimation (MLE) are commonly used to estimate parameters from observed data in wireless channels. However, these methods have limitations when dealing with intricate distributions, often requiring the use of nonlinear numerical techniques like nonlinear least squares (NLS) for estimation. The effectiveness of these methods often relies on the initial value chosen. Evolutionary algorithms (EAs) [4] are nonconventional approaches that have emerged as alternative methods to address these limitations. Unlike the NLS, they provide gradient-free procedures that can handle nondifferentiable fitness functions.

EAs are nature-inspired algorithms that establish a relation between Darwin's natural selection of biological evolution and complex optimization problem. The genetic algorithm (GA) [4] is the simplest EA applicable to several wireless communications problems, including joint channel and data estimation [5], user detection [6], and joint user detection and channel estimation [7], [8]. In terms of estimating wireless channel parameters, GA was used to estimate parameters in a multipath environment in [9], and has shown superior performance compared to traditional numerical methods for estimating Weibull parameters in [10]. Recent studies have also demonstrated the effectiveness of EAs in parameter estimation for $\alpha-\kappa-\mu$ fading channels [11]. However valuable, these analyses were based on simulated channel environments. Motivated by this drawback, we focus on using the GA for estimating practical channel parameters.

The main contributions are as follows. First, we present an extensive investigation on the applicability of the GA that uses mean squared error (MSE) and resistor-average distance (RAD) as fitness functions to estimate: 1) $\kappa-\mu$ and $\alpha-\mu$ parameters for small-scale fading; and 2) single-shadowed $\kappa-\mu$ Types I and II parameters for shadowed fading. Second, the estimations are applied to practical (real-world) mm-wave indoor distributed antenna system (DAS) measurements at 60 GHz. Finally, we compare the estimation performance of GA with the hybrid grey wolf and whale optimization algorithm (HGW-WOA), a recent meta-heuristic algorithm, leading to valuable insights. Choosing an appropriate estimation technique is crucial as different approaches can yield varying results for the same propagation environment, which can impact the conclusions drawn from the data. To our knowledge, the application of GAs to estimate fading parameters for real mm-wave propagation channels has

Samuel Borges Ferreira Gomes and Michel Daoud Yacoub are with the School of Electrical and Computer Engineering, University of Campinas, Campinas 13083-970, Brazil (e-mail: samuelbfgomes@gmail.com; mdyacoub@unicamp.br).

Nidhi Simmons and Simon L. Cotton are with the Centre for Wireless Innovation, Queen's University of Belfast, BT3 9DT Belfast, U.K. (e-mail: nidhi.simmons@qub.ac.uk; simon.cotton@qub.ac.uk).

Paschalis C. Sofotasios is with the Center for Cyber-Physical Systems, Department of Electrical Engineering and Computer Science, Khalifa University, Abu Dhabi, UAE (e-mail: paschalis.sofotasios@ku.ac.ae).

TABLE I
PDFs OF THE SINGLE SHADOWED $\kappa-\mu$ TYPES I AND II, $\kappa-\mu$ AND $\alpha-\mu$ FADING MODELS

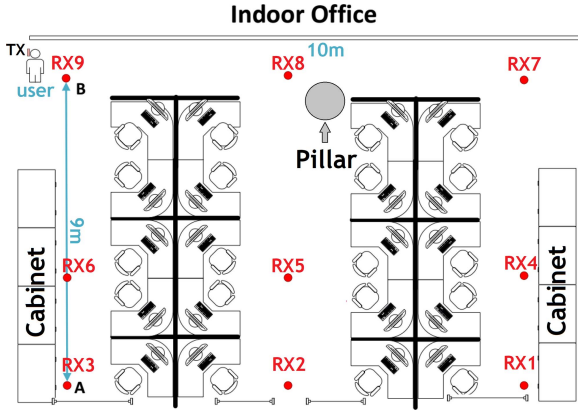| Fading models	PDFs
Single shadowed $\kappa-\mu$ Type I [16, eq 2]	$f_R(r) = \dfrac{2m_d^{m_d}(1+\kappa)^\mu \mu^\mu}{\Gamma(\mu)(m_d+\kappa\mu)^{m_d}} \dfrac{r^{2\mu-1}}{\bar{r}^{2\mu}} e^{-\frac{r^2(1+\kappa)\mu}{\bar{r}^2}} {}_1F_1\left(m_d;\mu;\dfrac{\mu^2\kappa(1+\kappa)r^2}{\bar{r}^2(m_d+\kappa\mu)}\right)$
Single shadowed $\kappa-\mu$ Type II [16, eq 6]	$f_R(r) = \dfrac{2(m_s-1)^{m_s}(1+\kappa)^\mu \mu^\mu r^{2\mu-1}\bar{r}^{2m_s} {}_2F_1\left(\frac{m_s+\mu}{2},\frac{1+m_s+\mu}{2};\mu;\frac{4\mu^2\kappa(1+\kappa)r^2\bar{r}^2}{[r^2(1+\kappa)\mu+\bar{r}^2(m_s-1+\kappa\mu)]^2}\right)}{B(m_s,\mu)[r^2(1+\kappa)\mu+\bar{r}^2(m_s-1+\kappa\mu)]^{m_s+\mu}}, \quad m_s > 1$
$\kappa-\mu$ [17, eq 11]	$f_R(r) = \dfrac{2\mu(1+\kappa)^{\frac{\mu+1}{2}}}{\bar{r}\kappa^{\frac{\mu-1}{2}}\exp(\mu\kappa)}\left(\dfrac{r}{\bar{r}}\right)^\mu \exp\left(-\mu(1+\kappa)\left(\dfrac{r}{\bar{r}}\right)^2\right)I_{\mu-1}\left(2\mu\sqrt{\kappa(1+\kappa)}\dfrac{r}{\bar{r}}\right)$
$\alpha-\mu$ [18, eq 1]	$f_R(r) = \dfrac{\alpha\mu^\mu r^{\alpha\mu-1}}{\bar{r}^{\alpha\mu}\Gamma(\mu)}\exp\left(-\mu\dfrac{r^\alpha}{\bar{r}^\alpha}\right)$

Indoor Office

Fig. 1.   MM-wave measurement set-up and environment [13].

not been explored in the literature. Similarly, the use of RAD as a fitness function.

II. PROPAGATION MEASUREMENTS AND FADING MODELS

1) mm-Wave Measurements: Fig. 1 shows an indoor DAS set-up. The red points denote the various ceiling locations in an office environment[1] where nine 60 GHz receiver (RX) boards were placed. A test user bearing a transmitter (TX) pretended to make a voice call while holding the device at their right ear. Two propagation scenarios were considered, namely, the user walking along paths AB and BA when the office area was unoccupied. As per [13], the TX transmitted a continuous wave signal with a power level of +10.9 dBm at 60.05 GHz. A v1.4 Red Pitaya data acquisition board recorded the received signal power. For more measurement details, see [13, Sec. II].

2) Shadowed and Small-Scale Fading Models: Shadowed and small-scale fading datasets were extracted from the received signal power measurement for analysis. As indicated in [13], before characterizing the fading observed at each receiver, the path loss was removed by fitting the log-distance path loss expression to the data [14]. The shadowing (or composite fading) was then extracted by applying a moving average window of ten lambda (10λ) length [15]. After implementing the above procedures, we are then left with the small-scale fading. Since the test user walked along two paths (AB and BA), and there are nine RXs, we have 18 datasets in total. Each of these 18 datasets were filtered to form small-scale and shadowed fadings. Hence, a total of 36 datasets were obtained and archived in [19]. Statistical characterization was performed using shadowed fading models

like the single shadowed $\kappa-\mu$ Types I and II [16], and small-scale fading models like the $\kappa-\mu$ [17] and $\alpha-\mu$ [18]. Table I presents their probability density functions (PDFs). Here, $\bar{r}$ is the root mean squared (rms) power of the signal envelope R, $\kappa > 0$ is the ratio of the total power of the dominant component to that of the scattered waves, $\alpha > 0$ captures the nonlinearity of the medium and $\mu > 0$ is related to the number of clusters. ${}_1F_1(a;b;z)$, and ${}_2F_1(a,b;c;z)$ denote confluent and Gauss hypergeometric functions, respectively. $I_\nu(\cdot)$ is the modified Bessel function of the first kind and order ν, $\Gamma(\cdot)$ is the Gamma function and $B(a,b)$ is the Beta function [20]. Finally, m_d and m_s denote the amount of shadowing experienced by the dominant component and scattered components, respectively. Since two distributions are characterized for each fading type, the total number of cases analyzed in this work is 72.

III. PARAMETER ESTIMATION METHODS

For the parameter estimation analysis, we assume that the data vector $\boldsymbol{R} = \{r_i, i = 1, 2, \ldots, n\}$ belongs to a set of n measured signal envelopes acquired from a population that hypothetically follows a given PDF, and is specified by the M-dimensional parameter $\boldsymbol{\theta} = \{\theta_m, m = 1, 2, \ldots, M\}$.

1) Nonlinear Least Squares: NLS is a well-established optimization technique that seeks to minimize the sum of squares of the residuals (difference between the observed and estimated values) [21]. To compute the estimates, starting points for the parameters are obtained using the MLE, which in this work were taken using the Rician and Nakagami-m distributions (particular cases of the considered PDFs).

2) Genetic Algorithms: Typically, a GA requires a *genetic representation* of the solution, and a *fitness function* to assess the solution. The *genetic representation* is given as an array of floating-point solutions that denote the parameters of the target PDFs. The *fitness function* $\mathcal{F}(\cdot)$ is defined over the genetic representation and assesses the quality of a given solution. It is used with the purpose of finding the parameter vector[2] $\hat{\boldsymbol{\theta}}$ that yields the highest fitness quality (lowest value) possible among empirical (true) and estimated PDFs. The algorithm then *generates* a population of solutions, which is refined by looping the *selection*, *crossover*, and *mutation* operators.

A population of N_P estimated parameters $\hat{\boldsymbol{\theta}} \in \mathbb{R}^M$ is *generated* randomly following an arbitrary uniform distributions. As a parent *selection* algorithm, the roulette wheel method [4] is employed. The roulette wheel is divided into slots with probabilities adding up to 1. Each slot is made proportional to the

---

[1]The exact details of the considered office environment can be found in [12].

[2]$\hat{\boldsymbol{\theta}} = \{\alpha,\mu,\bar{r}\}; \{\kappa,\mu,\bar{r}\}; \{\kappa,\mu,\bar{r},m_d\}; \{\kappa,\mu,\bar{r};m_s\}$; for α-μ, κ-μ, single shadowed κ-μ Types I and II, respectively.

fitness value of each individual, using the *fitness function* as a measure. A random selection point is chosen on the rim of the wheel. It is then repeatedly spun to choose parents based on the slot that lands at the point. Parents that have low fitness scores are more likely to be selected for reproduction. Unlike others, we propose using the RAD[3] [22] in the fitness function

$$\mathcal{F}_{\text{RAD}}(\boldsymbol{\theta}) = \left(1/\mathcal{P}(f, \hat{f}) + 1/\mathcal{P}(\hat{f}, f)\right)^{-1} \qquad (1)$$

where $\mathcal{P}(f, \hat{f}) = \int_{-\infty}^{\infty} f_R(r_i, \boldsymbol{\theta}) \log_2(f_R(r_i, \boldsymbol{\theta})/\hat{f}_R(r_i, \boldsymbol{\theta})) \, \mathrm{d}r$ is the KLD between the true PDF of the measured dataset $f_R(r_i, \boldsymbol{\theta})$ and estimated PDF $\hat{f}_R(r_i, \hat{\boldsymbol{\theta}})$. The corresponding MSE was also incorporated in $\mathcal{F}(\cdot)$ as [11]

$$\mathcal{F}_{\text{MSE}}(\boldsymbol{\theta}) = \mathbb{E}\left\{\sum_{i=1}^{n}\left[f_R(r_i, \boldsymbol{\theta}) - \hat{f}_R(r_i, \boldsymbol{\theta})\right]^2\right\} \qquad (2)$$

where $\mathbb{E}\{\cdot\}$ is the expectation operator. The GA looks for the value of $\hat{\boldsymbol{\theta}}$ that minimizes the MSE or RAD between the kernel density estimation (KDE) [23] of the measured signal sample set $f(\boldsymbol{R}, \boldsymbol{\theta})$, and estimated distribution[4] $\hat{f}(\boldsymbol{R}, \hat{\boldsymbol{\theta}})$.

Crossover is implemented through arithmetic recombination. Two offsprings are created from parents $\hat{\boldsymbol{\theta}}_{\boldsymbol{p_1}}, \hat{\boldsymbol{\theta}}_{\boldsymbol{p_2}} \in \mathbb{R}^M$, i.e., $\hat{\boldsymbol{\theta}}_{\boldsymbol{z_1}} = \beta\hat{\boldsymbol{\theta}}_{\boldsymbol{p_1}} + (1-\beta)\hat{\boldsymbol{\theta}}_{\boldsymbol{p_2}}$ and $\hat{\boldsymbol{\theta}}_{\boldsymbol{z_2}} = \beta\hat{\boldsymbol{\theta}}_{\boldsymbol{p_2}} + (1-\beta)\hat{\boldsymbol{\theta}}_{\boldsymbol{p_1}}$ [4], for some uniformly distributed $\beta \sim \mathcal{U}[-\gamma, 1+\gamma]$. These offsprings are then *mutated*. This involves generating random numbers from a normal distribution $\mathcal{N}(0, 1)$ in each element of the parameter vector $\hat{\boldsymbol{\theta}}_{\boldsymbol{z_i}}$, and comparing them to a fixed threshold p_M (mutation rate). If the generated number is below p_M, a value drawn randomly from a normal distribution with 0 mean and standard deviation σ is added to its corresponding element. The new offsprings replace two solutions with poor fitness quality in the population. This is repeated for a maximum number of generations[5] G, or until the difference between the best fitness function obtained at each iteration is less than 10^{-8}. Although the GA is not guaranteed to converge to a global optimum, it maintains a population of solutions agnostic from specific initialization. Thus, it provides a way to escape from the local optima, and cope with large and discontinuous search spaces [4]. This is a fundamentally different search to the Levenberg–Marquardt algorithm, which uses a trust region approach and adopted in NLS.

IV. COMPARING PARAMETER ESTIMATION METHODS

The usefulness of the GA to estimate parameters of the fading models is now verified by comparing it with the model fits obtained when using the traditional NLS. The second-order Akaike information criterion (AIC) is employed to estimate the quality of each model relative to the others, similar to the analysis in [24] and [25]. A smaller AIC value indicates a higher likelihood that the candidate model generated the dataset. In our analysis, we assume that if the AIC score computed using GA estimates (labeled as GA-MSE or GA-RAD based on the fitness function) is lower than that computed using the NLS estimates,

---

[3]RAD is a symmetric distance measure between two probability distributions, offering properties akin to the popular Kullback–Leibler divergence (KLD) but with the added advantage of satisfying the triangle inequality [22].

[4]Note that (1) and (2) represent the fitness functions that the optimization problem aims to minimize. To obtain the PDF from the measured samples, we have adopted a KDE on the linear-scale data of the measured signal with a Gaussian kernel and a fixed bandwidth of 0.05 [13].

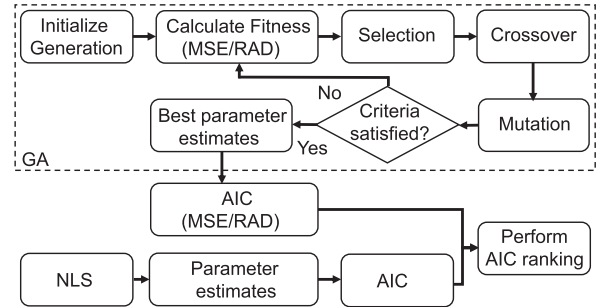[5]N_P is in the range 70–80, G in 500–600, γ, σ, and p_M in 0.2–0.3.

Fig. 2. Flowchart of GA along with the steps taken to compare GA and NLS.

TABLE II
ESTIMATED PARAMETERS FOR THE κ-μ, SINGLE SHADOWED κ-μ TYPES I AND II MODELS USING THE GA AND NLS

mm-wave link	Estimation method	κ-μ			AIC rank
		κ	μ	$\bar{r}$	
Path AB RX 1	GA: RAD	7.20	0.55	1.05	1
	GA: MSE	9.35	0.55	1.04	2
	NLS	69.99	0.08	1.04	3
		Single Shadowed κ-μ Type 1			AIC rank
		κ μ $\bar{r}$ m_d			
Path AB RX 8	GA: RAD	8.66 0.94 0.95 1.34			1
	GA: MSE	4.22 0.89 0.94 1.84			2
	NLS	4.20 0.89 0.94 1.84			2
		Single Shadowed κ-μ Type 2			AIC rank
		κ μ $\bar{r}$ m_s			
Path BA RX 5	GA: RAD	0.001 1.02 1.09 4.81			1
	GA: MSE	0.001 1.07 1.10 3.73			2
	NLS	0.001 1.07 1.10 3.72			2

then the GA estimates of the candidate model provide a better description of the dataset.[6] Fig. 2 shows the complete process of parameter estimation for both methods. The simulation code that supports our work can be found here [27].

Table II provides a sample of the 72 scenarios examined. It shows the parameters estimated using the two approaches along with their AIC ranks when the κ–μ PDF is fitted to the small-scale dataset for RX1 (path AB); and also when the single shadowed κ–μ Types I and II PDFs are fitted to the composite dataset for RX8 (path AB), and RX5 (path BA), respectively. The corresponding model fits are shown in Fig. 3(a)–(c), respectively. From these, it is clear that the GA is capable of estimating physically plausible fading parameters. For example, consider the parameters estimated via GA-RAD for the κ-μ model for RX1 (path AB). Although there existed a strong dominant signal component ($\kappa > 1$), it is observed that the received signals experienced considerable fading ($\mu < 1$). Furthermore, the model estimates obtained using the GA-RAD provide the best fit to the dataset, possibly because RAD makes use of rigorous information theory methods to describe probability and information distances. Thus, it has precise theoretic distance interpretations within this branch of mathematics (e.g., [28, Th. 5.4.3]). The superior fit provided by GA-RAD is visible at the lower and upper tails of the empirical PDFs. Similar conclusions can be drawn from the AIC rankings (that depends on the AIC computed) in Table II.

The estimated parameters for all models using both methods along with their AIC ranks, can be found in [29]. We observe

---

[6]Another goodness-of-fit test called the Bayesian information criterion [26] (BIC) was also implemented in a similar manner to the AIC. The results were in agreement with the AIC results obtained and discussed in Section IV.
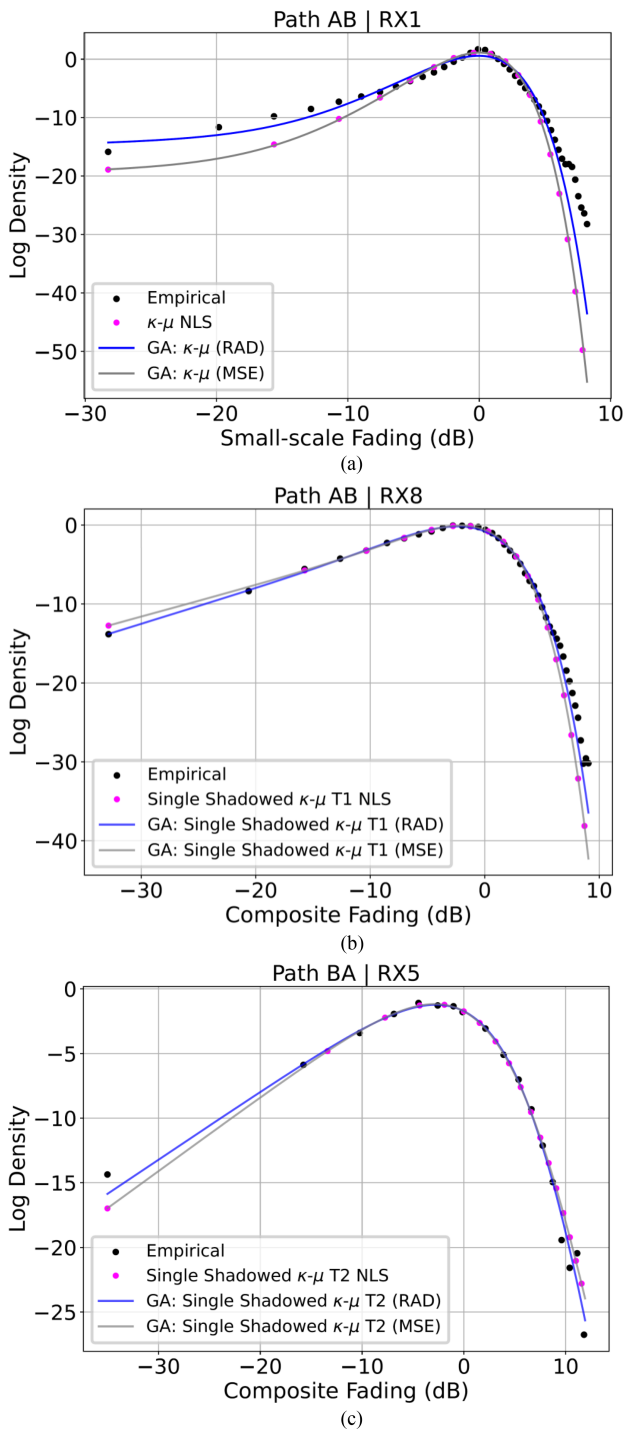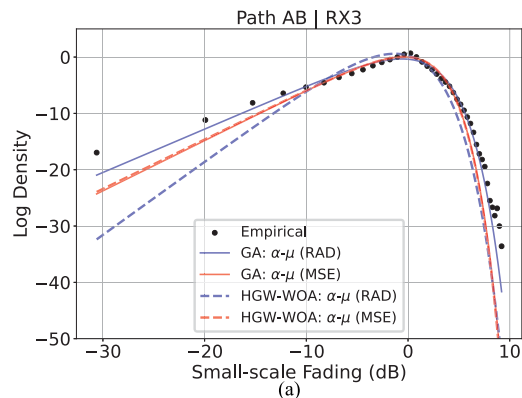
Fig. 3. Empirical versus theoretical probability densities for the (a) κ–μ, (b) single shadowed κ–μ Type 1, and (c) single Shadowed κ–μ Type 2 models. Here the model parameters are estimated using NLS and GA. See Table II.

Fig. 4. Empirical versus theoretical probability densities for the (a) α–μ model. (b) Model parameters estimated using GA and HGW-WOA.

in 85% of all tested scenarios; performed similarly to the NLS in 14% of the cases and was slightly worse than the NLS in 1% of the tested cases.

To better contextualize the use of the GA within the meta-heuristic family of algorithms, a modern meta-heuristic approach called the HGW-WOA [30] was explored. The HGW-WOA is a hybrid swarm-based technique inspired by the social hierarchy and hunting behavior of gray wolves and the feeding behavior of humpback whales, in contrast to the evolution-based GA. The estimated parameters obtained using the HGW-WOA can be found in [31]. Fig. 4 shows an example of the GA performing better than this algorithm. Here, the α-μ PDF was fitted to the small-scale dataset for RX3 (path AB), while Fig. 4(b) shows the corresponding parameters estimated. Overall, it was found that the GA performed better than the HGW-WOA in 72% of the scenarios; exhibited a similar performance in 15% of the cases, and performed marginally worse than HGW-WOA in 13% of the tested scenarios.[7] Thus, among the two meta-heuristic algorithms, the GA was found to be more suited for parameter estimation of fading distributions.

V. CONCLUSION

This letter showcased the significant potential of the GA for channel parameter estimation in real propagation studies. When compared using the goodness-of-fit technique, GA outperformed NLS in the vast majority of the mm-wave scenarios, particularly with RAD as the fitness function. Furthermore, GA demonstrated better performance when compared to HGW-WOA (a more recent meta-heuristic approach). Thus, the GA stands out as a prominent meta-heuristic algorithm for parameter estimation in future propagation studies.

[7]The effectiveness of an optimization algorithm varies based on the problem's complexity and characteristics. Certain algorithms are better suited to specific problems due to their inherent search strategies. The fading parameter estimation problem's specific nature and the presence of particular features in the search space (e.g., problem regularity and convergence behavior) may have favored GA's search mechanisms.

that the parameters estimated via the GA outperformed NLS estimates for all four fading models across the vast majority of tested cases, e.g., for the α–μ model, the GA estimates described the dataset better than the NLS estimates in 94% of the cases, and for the κ–μ, single shadowed κ–μ Type I, and single shadowed κ–μ Type II models, the GA estimates described the dataset better than the NLS estimates in 89%, 72%, and 83% of the tested cases, respectively. Overall, the GA outperformed NLS

References

[1] S. Geng, J. Kivinen, X. Zhao, and P. Vainikainen, "Millimeter-wave propagation channel characterization for short-range wireless communications," *IEEE Trans. Veh. Technol.*, vol. 58, no. 1, pp. 3–13, Jan. 2009.

[2] S. Rangan, T. S. Rappaport, and E. Erkip, "Millimeter-wave cellular wireless networks: Potentials and challenges," *Proc. IEEE*, vol. 102, no. 3, pp. 366–385, Mar. 2014.

[3] S. Collonge, G. Zaharia, and G. Zein, "Influence of the human activity on wide-band characteristics of the 60 GHz indoor radio channel," *IEEE Trans. Wireless Commun.*, vol. 3, no. 6, pp. 2396–2406, Jun. 2004.

[4] A. E. Eiben and J. E. Smith, *Introduction to Evolutionary Computing*, 2nd ed. Berlin, Germany: Springer, 2015.

[5] S. Chen and Y. Wu, "Maximum likelihood joint channel and data estimation using genetic algorithms," *IEEE Trans. Signal Process.*, vol. 46, no. 5, pp. 1469–1473, May 1998.

[6] C. Ergun and K. Hacioglu, "Multiuser detection using a genetic algorithm in CDMA communications systems," *IEEE Trans. Commun.*, vol. 48, no. 8, pp. 1374–1383, Aug. 2000.

[7] K. Yen and L. Hanzo, "Genetic algorithm assisted joint multiuser symbol detection and fading channel estimation for synchronous CDMA systems," *IEEE J. Sel. Areas Commun.*, vol. 19, no. 6, pp. 985–998, Jun. 2001.

[8] T.-H. Tan, Y.-F. Huang, L.-C. Hsu, and C.-H. Wu, "Joint channel estimation and multi-user detection for MC-CDMA system using genetic algorithm and simulated annealing," in *Proc. IEEE Int. Conf. Syst. Man Cybern.*, 2010, pp. 249–256.

[9] A. Ebrahimi and A. Rahimian, "Estimation of channel parameters in a multipath environment via optimizing highly oscillatory error functions using a genetic algorithm," in *Proc. 15th Int. Conf. Softw. Telecommun. Comput. Netw.*, 2007, pp. 1–5.

[10] M. B. Koca, M. B. Kilic, and Y. Şahin, "Using genetic algorithms for estimating Weibull parameters with application to wind speed," *An Int. J. Optim. Control: Theories Appl.*, vol. 10, no. 1, pp. 137–146, Feb. 2020. [Online]. Available: http://www.ijocta.org/index.php/files/article/view/741

[11] C. Lemos, A. Veiga, and S. Fasolo, "Estimation of α-κ-μ mobile fading channel parameters using evolutionary algorithms," *Telecommun. Syst.*, vol. 77, pp. 189–211, 2021.

[12] S. K. Yoo, S. L. Cotton, R. W. Heath, and Y. J. Chun, "Measurements of the 60 GHz UE to eNB channel for small cell deployments," *IEEE Wireless Commun. Lett.*, vol. 6, no. 2, pp. 178–181, Apr. 2017.

[13] L. Zhang, S. K. Yoo, and S. L. Cotton, "A measurements based characterization of fading in indoor millimeter-wave distributed antenna systems," in *Proc. IEEE Int. Symp. Antennas Propag. USNC-URSI Radio Sci. Meeting*, 2019, pp. 2077–2078.

[14] N. Jalden, P. Zetterberg, B. Ottersten, A. Hong, and R. Thoma, "Correlation properties of large scale fading based on indoor measurements," in *Proc. IEEE Wireless Commun. Netw. Conf.*, 2007, pp. 1894–1899.

[15] L. Zhang, Y. Hua, S. L. Cotton, S. K. Yoo, C. R. C. M. Da Silva, and W. G. Scanlon, "An RSS-based classification of user equipment usage in indoor millimeter wave wireless networks using machine learning," *IEEE Access*, vol. 8, pp. 14928–14943, 2020.

[16] N. Simmons, C. R. N. D. Silva, S. L. Cotton, P. C. Sofotasios, S. K. Yoo, and M. D. Yacoub, "On shadowing the κ-μ fading model," *IEEE Access*, vol. 8, pp. 120513–120536, Jun. 2020.

[17] M. Yacoub, "The κ-μ distribution and the η-μ distribution," *IEEE Antennas Propag. Mag.*, vol. 49, no. 1, pp. 68–81, Feb. 2007.

[18] M. D. Yacoub, "The α-μ distribution: A physical fading model for the Stacy distribution," *IEEE Trans. Veh. Technol.*, vol. 56, no. 1, pp. 27–34, Jan. 2007.

[19] "mm-Wave Datasets," [Online]. Available: https://github.com/ML4Comms/ga-mmwave/tree/master/datasets

[20] I. S. Gradshteyn and I. M. Ryzhik, *Table of Integrals, Series, and Products*, 7th ed. San Francisco, CA, USA: Elsevier/Academic, 2007.

[21] J. E. Dennis, "Nonlinear least squares," in *State of the Art in Numerical Analysis*, D. Jacobs, Ed., San Francisco, CA, USA: Academic, 1977, pp. 269–312.

[22] D. H. Johnson and S. Sinanovic, "Symmetrizing the Kullback-Leibler distance," *IEEE Trans. Inf. Theory*, Feb. 2000.

[23] A. Z. Zambom and R. Dias, "A review of kernel density estimation with applications to econometrics," 2012.

[24] A. Fort, C. Desset, P. De Doncker, P. Wambacq, and L. Van Biesen, "An ultra-wideband body area propagation channel model-from statistics to implementation," *IEEE Trans. Microw. Theory Techn.*, vol. 54, no. 4, pp. 1820–1826, Jun. 2006.

[25] S. K. Yoo, S. Cotton, P. Sofotasios, M. Matthaiou, M. Valkama, and G. Karagiannidis, "The Fisher-Snedecor F distribution: A simple and accurate composite fading model," *IEEE Commun. Lett.*, vol. 21, no. 7, pp. 1661–1664, Jul. 2017.

[26] P. Stoica and Y. Selén, "Model-order selection: A review of information criterion rules," *IEEE Signal Process. Mag.*, vol. 21, no. 4, pp. 36–47, Jul. 2004.

[27] "Simulation code," [Online]. Available: https://github.com/ML4Comms/ga-mmwave/tree/master/

[28] M. Thomas and A. T. Joy, *Elements of Information Theory*. New York, NY, USA: Wiley, 2006.

[29] "GA and NLS AIC ranks," [Online]. Available: https://github.com/ML4Comms/ga-mmwave/blob/master/results/Final%20Results%20GA%20vs.%20NLS.xlsx

[30] O. O. Obadina, M. A. Thaha, K. Althoefer, and M. H. Shaheed, "Dynamic characterization of a master–slave robotic manipulator using a hybrid grey wolf–whale optimization algorithm," *J. Vib. Control*, vol. 28, no. 15/16, pp. 1992–2003, Mar. 2022, doi: 10.1177/10775463211003402.

[31] "GA and HGW-WOA AIC ranks," [Online]. Available: https://github.com/ML4Comms/ga-mmwave/blob/master/results/Final%20Results%20GA%20vs.%20HGW-WOA.xlsx